

1 **Short Title:**

2 Targets of the flowering time regulator FD

3

4 **Author for Contact:**

5 Markus Schmid

6

7 **Article title:**

8 FT modulates genome-wide DNA-binding of the bZIP transcription factor FD in
9 *Arabidopsis thaliana*

10

11 **Author names:**

12 Silvio Collani^{1,2}, Manuela Neumann², Levi Yant^{2,#}, Markus Schmid^{1,2,3,*}

13

14 **Author affiliations:**

15 ¹Umeå Plant Science Centre, Department of Plant Physiology, Umeå University, SE-
16 901 87 Umeå, Sweden.

17 ²Max Planck Institute for Developmental Biology, Department of Molecular Biology,
18 72076 Tübingen, Germany.

19 ³Beijing Advanced Innovation Centre for Tree Breeding by Molecular Design, Beijing
20 Forestry University, Beijing 100083, People's Republic of China.

21

22 **One sentence summary:**

23 Genomic and biochemical analyses identify targets of the flowering time regulator FD
24 at the genome-wide scale and shed light on the requirement for interaction with the
25 florigen FLOWERING LOCUS T.

26

27 **Author contributions:**

28 S.C., L.Y., and M.S. designed the experiments. L.Y. established some of the FD:GFP
29 reporter lines and performed initial ChIP (-seq) and flowering time analyses. M.N.
30 cloned phosphomic and non-phosphorable versions of FD and analyzed their effect on
31 flowering time. S.C. performed the EMSA studies, flowering times analysis and carried
32 out and analyzed the ChIP-seq and RNA-seq experiments. S.C. and M.S. wrote the
33 manuscript with input from all authors. M.S. agrees to serve as the corresponding
34 author.

35

36 **Funding information:**

37 Supported through the Sonderforschungsbereich 1101 (Collaborative Research Centre
38 1101) project grant SFB1101/1-B04 and a research project grant from the Knut and
39 Alice Wallenberg Foundation (2016.0025) to M.S.

40

41 **Present Address**

42 #School of Life Sciences and Future Foods Beacon of Excellence, University of
43 Nottingham, United Kingdom.

44

45 **E-mail address of Author for Contact:**

46 markus.schmid@umu.se

47

48 **ABSTRACT**

49 The transition to flowering is a crucial step in the plant life cycle that is controlled by
50 multiple endogenous and environmental cues, including hormones, sugars,
51 temperature, and photoperiod. Permissive photoperiod induces the expression of
52 *FLOWERING LOCUS T (FT)* in the phloem companion cells of leaves. The FT protein
53 then acts as a florigen that is transported to the shoot apical meristem (SAM), where it
54 physically interacts with the bZIP transcription factor FD and 14-3-3 proteins.
55 However, despite the importance of FD for promoting flowering, its direct
56 transcriptional targets are largely unknown. Here, we combined ChIP-seq and RNA-
57 seq to identify targets of FD at the genome scale and assess the contribution of FT to
58 DNA binding. We further investigated the ability of FD to form protein complexes with
59 FT and TFL1 through the interaction with 14-3-3 proteins. Importantly, we observe
60 direct binding of FD to targets involved in several aspects of plant development not
61 understood to be directly related to the regulation of flowering time. Our results confirm
62 FD as central regulator of the floral transition at the shoot meristem and provides
63 evidence for crosstalk between the regulation of flowering and other signaling
64 pathways.

65

66

67

68 **INTRODUCTION**

69 The floral transition represents a crucial checkpoint in the plant life cycle at which the
70 shoot apical meristem (SAM) ceases to produce only leaves and begins producing
71 reproductive organs. As the commitment to this developmental phase transition is
72 usually irreversible for a given meristem, plants have evolved several pathways to
73 integrate environmental and endogenous stimuli to ensure flowering is induced at the
74 correct time. A rich literature has identified hormones, sugars, temperature, and day
75 length (photoperiod) as main factors in flowering time regulation (reviewed in Srikanth
76 and Schmid, 2011; Romera-Branchat et al., 2014; Song et al., 2015). Photoperiod in
77 particular has been shown to regulate flowering time in many plant species and,
78 depending on the light requirements, short day (SD), long day (LD) and day-neutral
79 plants have been distinguished. In *Arabidopsis thaliana*, LD promotes flowering but
80 plants will eventually flower even under non-inductive SD.

81 It has long been known that in day-length responsive species, inductive photoperiod is
82 mainly perceived in leaves where it results in the formation of a long-distance signal,

83 or florigen, that moves to the SAM to induce the transition to flowering (An et al., 2004;
84 Corbesier et al., 2007; Mathieu et al., 2007). The molecular nature of florigen has
85 eluded identification for the better part of a century. However, recently *FLOWERING*
86 *LOCUS T (FT)* and related genes, which encode phosphatidylethanolamine-binding
87 proteins (PEBP), have been identified as evolutionarily conserved candidates
88 (Corbesier et al., 2007; Mathieu et al., 2007). Under inductive photoperiod, *FT* is
89 expressed in leaf phloem companion cells (PCC) and there is good evidence that the FT
90 protein is loaded into the phloem sieve elements and transported to the SAM (reviewed
91 in Srikanth and Schmid, 2011; Song et al., 2015). At the SAM, FT interacts with FD
92 and 14-3-3 proteins and the resulting florigen-activation complex (FAC) is thought to
93 control the correct expression of flowering time and floral homeotic genes to promote
94 the transition of the vegetative meristem into a reproductive inflorescence meristem
95 (Abe et al., 2005; Wigge et al., 2005; Taoka et al., 2011).

96 FD belongs to the bZIP transcription factor (TF) family (Jakoby et al., 2002) and is
97 mainly expressed at the SAM (Abe et al., 2005; Schmid et al., 2005; Wigge et al., 2005).
98 It has been proposed that, in order to interact with FT and 14-3-3 proteins, FD must be
99 phosphorylated at threonine 282 (T282) (Abe et al., 2005; Wigge et al., 2005; Taoka et
100 al., 2011). Recently, two calcium-dependent kinases expressed at the SAM, CALCIUM
101 DEPENDENT PROTEIN KINASE 6 (CPK6) and CPK33, have been shown to
102 phosphorylate FD (Kawamoto et al., 2015). FD interacts not only with FT but also with
103 other members of the PEBP protein family. Interestingly, some of the six PEBP proteins
104 encoded in the *A. thaliana* genome regulate flowering in opposition (Kim et al., 2013).
105 FT and its paralog TWIN SISTER OF FT (TSF) promote flowering. Mutations in *tsf*
106 enhance the late flowering phenotype of *ft* in LD, but in addition *TSF* also has distinct
107 roles in SD (Yamaguchi et al., 2005). Other members of the PEBP protein family, most
108 prominently TERMINAL FLOWER 1 (TFL1), oppose the flower-promoting function
109 of FT and TSF, and repress flowering. The Arabidopsis ortholog of
110 CENTRORADIALIS (ATC) has been shown to act as a SD-induced floral inhibitor
111 that is expressed mostly in the vasculature, but was undetectable at the SAM (Huang et
112 al., 2012). Furthermore, ATC has been suggested to move long distances and can
113 interact with FD to inhibit *APETALAI (API)* expression. ATC has thus been proposed
114 to antagonize the flower-promoting effect of FT (Huang et al., 2012). Similarly,
115 orthologs of ATC in rice (RCNs) have been recently showed to antagonize the function
116 of FT-like protein (Kaneko-Suzuki et al., 2018). Finally, BROTHER OF FT (BFT),
117 which like *ATC* is strongly expressed in the leaf vasculature, can interact with FD in

118 the nucleus, interfering with FT function under high salinity by inhibiting *API*
119 expression, thereby delaying flowering (Yoo et al., 2010; Ryu et al., 2014).

120 TFL1 differs from FT only in 39 non-conserved amino acids but as mentioned above
121 has an opposite biological function: TFL1 represses flowering while FT is a floral
122 promoter (Ahn et al., 2006). It has been demonstrated that substitutions of a single
123 amino acid (TFL1-H88; FT-Y85) or exchange of the segment B encoded by the fourth
124 exon are sufficient to impose TFL1-like activity onto FT, and *vice versa* (Hanzawa et
125 al., 2005; Ahn et al., 2006; Ho and Weigel, 2014). Similar to FT, TFL1 also interacts
126 with FD, both in yeast-2-hybrid assays as well as in plant nuclei (Wigge et al., 2005;
127 Hanano and Goto, 2011). Together, these findings suggest that activating FD-FT and
128 repressive FD-TFL1 complexes compete for binding to the same target genes (Ahn et
129 al., 2006). This hypothesis is further supported by the observation that TFL1 apparently
130 acts to repress transcription (Hanano and Goto, 2011) whereas FT seems to function as
131 a transcriptional (co-)activator (Wigge et al., 2005). However, evidence that these
132 protein complexes in fact share interactors such as 14-3-3 proteins or control the same
133 targets remains sparse.

134 FD has been reported as direct and indirect regulator of important flowering time and
135 floral homeotic genes such as *SUPPRESSOR OF OVEREXPRESSION OF CONSTANS*
136 *1 (SOC1)*, *SQUAMOSA PROMOTER BINDING PROTEIN-LIKE 3 (SPL3)*, *SPL4*,
137 *SPL5*, *LEAFY (LFY)*, *API*, and *FRUITFULL (FUL)*. Several flowering time pathways
138 contribute to *SOC1* regulation. Indeed, it has been proposed that expression of *SOC1*
139 can be directly promoted by the FD-FT complex (Lee and Lee, 2010). However, *SOC1*
140 expression can also be activated independently from FD-FT probably through the
141 *SPL3*, *SPL4*, and *SPL5* proteins (Moon et al., 2003; Wang et al., 2009; Lee and Lee,
142 2010), which have been shown to be directly or indirectly activated by the FD-FT
143 complex (Jung et al., 2012). The activation of floral homeotic genes such as *API* and
144 *FUL* in response to FD-FT activity at the SAM can at least in part be explained by the
145 direct activation of the floral meristem identity gene *LFY* through *SOC1* (Moon et al.,
146 2005; Yoo et al., 2005; Jung et al., 2012). In addition, it has also been proposed that the
147 FD-FT complex can promote the expression of *API* and *FUL* by directly binding to
148 their promoters (Abe et al., 2005; Teper-Bamnolker and Samach, 2005; Wigge et al.,
149 2005). Taken together, these results support a central role for FD in integrating different
150 pathways to ensure the correct timing of flowering. However, FD targets have not yet
151 been identified at the genome scale, nor has the requirement for protein complex
152 formation for FD function in *A. thaliana* been addressed systematically.

153 Here we identify direct and indirect targets of FD at the genome scale using ChIP-seq
154 and RNA-seq in wildtype as well as in *ft-10 tsf-1* double mutants. Our results
155 demonstrate that FD can bind to DNA *in vivo* even in the absence of FT/TSF. However,
156 FD binding to a subset of targets, which includes many important flowering time and
157 floral homeotic genes, was reduced in the *ft-10 tsf-1* double mutant, strongly supporting
158 a role for FT/TSF in modulating the binding of FD to DNA and the expression of
159 functionally important target genes. In addition, we report the effects of FD
160 phosphorylation on protein complex formation with FT and TFL1 via 14-3-3 proteins
161 *in vitro* and show how phosphorylation of FD affects flowering time *in planta*. Finally,
162 our ChIP-seq experiments identified hundreds of previously unknown FD target genes,
163 both in the PCCs as well as at the SAM. For example, we observed that FD directly
164 binds to and regulates the expression of genes in hormone signaling pathways. These
165 newly identified FD target genes represent a precious resource not only to enhance our
166 knowledge of the photoperiod pathway but also to better understand the integration of
167 different signaling pathways at the transcriptional level. Taken together, our findings
168 support a role for FD as a central integrator of flowering time and provide important
169 novel data to guide future research on the integration of diverse signaling pathways at
170 the SAM.

171

172

173

174 **RESULTS**

175 **FD binds G-box motifs when expressed in PCCs**

176 FD is normally expressed at the shoot apical meristem (SAM) whereas its interaction
177 partner FT is expressed in leaf phloem companion cells (PCC). As most 14-3-3 proteins
178 are ubiquitously expressed at moderate to high levels and have also been detected in
179 PCCs (Schmid et al., 2005; Deeken R. et al., 2008), we reasoned that expression of FD
180 from the PCC-specific *SUC2* promoter would maximize FAC complex formation and
181 enable us to investigate the role of FT in modulating FD transcriptional activity.

182 We performed ChIP-seq on independent biological duplicates in a stable
183 *pSUC2::GFP:FD* reporter line, which shows no discernible phenotype when
184 comparted to Col-0 background. A *pSUC2::GFP:NLS* line, in which the GFP protein
185 is fused to the nuclear localization signal (NLS) was used as a control. A total of 2068
186 and 3236 genomic regions showing significant enrichment (peaks) were identified in
187 the first and second replicate, respectively (Fig. S1A).

188 In the individual replicates, the majority of the peaks mapped to promoter regions
189 (65.1% and 63.8%, respectively), followed by intergenic regions (16% and 16.8%),
190 transcriptional terminator sites (9.2% and 10.7%), exons (6.4% and 5.6%) introns
191 (2.4% and 2.3%), 5'-UTRs (0.5% and 0.3%), and 3'-UTRs (0.4% and 0.5%) (S1D).

192 The relative enrichment of peaks mapping to promoter regions is in agreement with
193 what is expected from a transcriptional regulator. In both replicates, the majority of the
194 peaks are located between 600 bp and 300 bp upstream the nearest transcription start
195 site (TSS) (Fig. S1G, J). Overlapping results from the two biological replicates
196 identified 1754 high-confidence peaks shared in both experiments (Fig. S1A,
197 Supplemental Data Set 1). Similar to the individual experiments, these high-confidence
198 peaks mostly mapped to the promoter regions (66.8%) (Fig. 1A). Only this subset of
199 peaks, which includes important flowering time and flower development genes such as
200 *API*, *FUL*, *LFY*, *SOC1*, *SEP1*, *SEP2*, *SEP3*, was used for further analysis.

201 *De novo* motif analysis of the 1754 high-confidence peaks using MEME-ChIP
202 (Machanick and Bailey, 2011) revealed that peak regions showed a strong enrichment
203 of G-boxes (CACGTG), which is a canonical bZIP binding site (Fig. S1M). The subset
204 of 1754 peak regions was associated with 1676 unique genes, with 68 genes containing
205 more than one FD binding site. Taken together, these results demonstrate that, when
206 misexpressed in the PCCs, FD is capable of binding to G-box elements in a large
207 number of genes that are involved in diverse aspects of the plant life cycle.

208

209 **FT and TSF enhance binding of FD to DNA**

210 To test whether FT and its paralog TSF are required for FD to bind to DNA, the
211 *pSUC2::GFP:FD* reporter and *pSUC2::GFP:NLS* control constructs were transformed
212 into the *ft-10 tsf-1* mutant background. Results from two independent biological
213 replicates show that FD is capable of binding to DNA even in the absence of *FT* and
214 *TSF*. Most peaks (63% and 62.1% in the first and second biological replicate,
215 respectively) mapped to promoter regions within 600 bp and 300 bp nucleotides
216 upstream the nearest TSS (Fig. S1E, H, K). Overall, these results are very similar to
217 those observed for *pSUC2::GFP:FD* in Col-0 (Fig. 1A, Fig. S1E, H, K, N). Comparison
218 between the two biological replicates identified 2696 common peaks in *ft-10 tsf-1*
219 mutant that mapped to 2504 unique genes (Fig. S1B, Supplemental Data Set 2).

220 Surprisingly, overlapping the sets of genomic regions bound by FD with high-
221 confidence in WT (1754) and *ft-10 tsf-1* (2696) backgrounds identified 1530 shared
222 peaks (Fig. 1B, Supplemental Data Set 3), suggesting that FD is capable of binding to

223 the majority of its targets in the absence of FT and TSF. Motif enrichment analysis of
224 sequence comprising the 1530 shared peaks revealed that FD maintained a strong
225 preference for binding to G-box motifs (Fig. 1C).

226 Analysis of differentially bound (DB) regions revealed that, although FT and TSF were
227 not required for FD to bind DNA, their presence increased the enrichment of FD on a
228 subset of target loci and this difference in binding was sufficient to discriminate Col-0
229 and *ft-10 tsf-1* (Fig. 1D). A total of 885 DB regions with a FDR < 0.05 were observed
230 between WT and *ft-10 tsf-1* and almost all of these loci showed higher enrichment in
231 WT (Fig. 1E, Supplemental Data Set 4). Interestingly, this subset includes important
232 floral homeotic genes such as *API*, *SEP1*, *SEP2*, and *FUL*, as well as two members of
233 the *SPL* gene family, *SPL7* and *SPL8*. We also found FD bound to the second exon of
234 *LFY*, a master regulator of flower development (Fig. 1F). In addition, we detected
235 binding to loci encoding genes involved in the regulation of gibberellic acid
236 biosynthesis and degradation such as *GA2OX4*, *GA2OX6*, and *GA3OX1* as well as to
237 three key components of the circadian clock, *CCA1*, *LHY*, and *TIC* (Supplemental Data
238 Set 4).

239 To test the robustness of our results and for any possible bias due to the use of the
240 different genetic backgrounds Col-0 and *ft-10 tsf-1* as controls, peaks were called again
241 using *pSUC2::GFP:NLS* in Col-0 as single negative control. Analysis identified 917
242 DB loci (Fig. S2), which is comparable to the 885 DB loci from the previous analysis
243 (Fig. 1E). In addition, affinity test analysis clustered by genotype rather than the control
244 used (Fig. S2), ruling out strong bias due to the usage of different genetic backgrounds
245 for peak calling.

246 Importantly, FD is capable of inducing the known FAC target gene *API* in leaves when
247 expressed under the *pSUC2* promoter, suggesting that a functional FAC can be formed
248 in the phloem companion cells when FD is present (Fig. S3A). The finding that *API*
249 expression could only be observed in the Col-0 background but not in *pSUC2::GFP:FD*
250 *ft-10 tsf-1* further supports this idea. However, in contrast to *API*, we failed to detect
251 induction of *SOCl* in the PCCs of *pSUC2::GFP:FD* (Fig.S3A), suggesting that other
252 co-factor(s) are specifically expressed at the SAM might be required to fully activate
253 FD target gene expression.

254

255 **FD phosphorylation is required for complex formation and to promote flowering**

256 To confirm the binding of FD to G-boxes we performed electrophoretic mobility shift
257 assays (EMSAs) using the bZIP domain of the *A. thaliana* FD protein (FD-C) and a

258 probe consisting of a 30bp fragment from the *SEP3* promoter containing a G-box that
259 we had identified as FD target region in our ChIP-seq (Fig. 1F). We observed weak
260 binding of FD-C, but failed to detect higher order complexes when 14-3-3, FT, or both
261 were added (Fig. 2A). In contrast, a clear supershift with 14-3-3 and FT was observed
262 when a phosphomimic variant of FD-C, FD-C_T282E, was used (Fig. 2B).
263 Interestingly, TFL1, which is similar to FT in structure (Ahn et al., 2006) but delays
264 flowering, was capable of forming a complex with 14-3-3 and wildtype FD-C (Fig. 2A).
265 Similar results were obtained with the full-length version of FD (Fig. S4A). Taken
266 together, these results demonstrate that *A. thaliana* FD is capable of binding to DNA
267 without FT, confirming results from our ChIP-seq experiments. Furthermore, this
268 indicates that the unphosphorylated form of FD, in complex with 14-3-3 proteins, can
269 interact with TFL1.

270 To investigate the importance of FD phosphorylation *in vivo* we complemented the *fd-*
271 *2* mutant with *pFD::FD*, *pFD::FD-T282E*, and *pFD::FD-T282A* (which cannot be
272 phosphorylated) and determined flowering time of homozygous transgenic plants.
273 Plants transformed with the WT version of FD rescued the late flowering phenotype of
274 *fd-2*, indicating that the rescue construct was fully functional (Fig. 3). In contrast, plants
275 transformed with the T282A version flowered with the same number of leaves as *fd-2*,
276 demonstrating that FD needs to be phosphorylated to induce flowering. Interestingly,
277 plants transformed with the T282E phosphomimic version of FD flowered even earlier
278 than WT (Fig. 3), indicating that control of FD phosphorylation is important for its
279 function *in vivo*. To test whether serine 281 (S281), which is located next to T282,
280 constitutes a potential FD phosphorylation site, we complemented *fd-2* with *pFD::FD-*
281 *S281E* and *pFD::FD-S281E/T282E* constructs. Interestingly, these lines flowered as
282 early as plants transformed with the phosphomimic version T282E (Fig. 3), indicating
283 that S281 may be a FD phosphorylation site but that mimicking double-phosphorylation
284 of S281/T282 does not accelerate flowering any further. These *in vivo* results are in
285 agreement with our *in vitro* EMSA results and confirm that phosphorylation of FD is
286 required for its function and must be finely regulated in order to avoid either premature
287 or delayed flowering. It should be noted, however, that the phosphomimic version of
288 the C-terminal fragment of FD (as used in the EMSA analyses) is insufficient to fully
289 rescue the late flowering of *fd-2* (Fig. S3B), suggesting that the N-terminal region of
290 FD, even though it does not contain any known functional domains, nevertheless
291 contributes to FD function.

292

293 **Targets of FD at the SAM**

294 The rationale for carrying out the initial ChIP-seq experiments in PCCs was to
295 maximize the likelihood of FAC formation and to study the contribution of FT/TSF to
296 FD DNA binding. However, since our ChIP-seq and EMSA results indicated that FD-
297 FT interaction is not required for FD to bind to DNA, we decided to determine direct
298 targets of FD in its natural context at the SAM.

299 To this end we performed ChIP-seq using a *fd-2* mutant complemented with a
300 *pFD::GFP:FD* construct (Fig. S3C). We performed ChIP-seq using two independent
301 biological replicates from apices of 16-day-old plants grown in LD conditions. In the
302 two replicates, we could identify 703 and 1222 FD-bound regions, respectively, of
303 which 595 were shared between the replicates (Fig. S1C, Supplemental Data Set 5). Of
304 these, 69.7% mapped to core promoter regions within 300 to 600 bp upstream of the
305 nearest TSS, 15.8% to intergenic regions, followed by lesser percentages to TTS
306 (6.2%), exons (5.9%), introns (1.8%) and 5'-UTRs (0.5%) (Fig. 1G, Fig. S1F, I, L).
307 Similar to the situation in our PCC-specific ChIP-seq analyses we found G-box
308 sequences as the most overrepresented transcription factor binding sites under the peak
309 regions (Fig. 1H, Fig. S1O). The 595 peak regions shared between the replicates
310 mapped to 572 individual genes, which we consider high-confidence *in vivo* targets of
311 FD at the SAM and include important flowering-related genes such as *API*, *FUL*,
312 *SOC1*, and *SEP3*.

313 The precise location of the FD binding site in the *API* promoter has been discussed
314 controversially (Wigge et al., 2005; Benlloch et al., 2011). Taking into account all six
315 ChIP-seq datasets, we were able to extract a 64 bp sequence covering the peak summits
316 on the *API* promoter (Fig. 4A, B). Interestingly, this sequence lies about 100 bp
317 downstream of the C-box that had previously been implicated in FD binding to *API*
318 (Wigge et al., 2005), but contains several other palindromic sequences. However, none
319 of these sequences is a *bona fide* G-box. We selected three potential binding sites within
320 the 64 bp sequence and tested them, along with the upstream C-box, by EMSA for FD
321 binding (Fig. 4C, S4B). Results show that only the phosphomimic version of FD-C
322 (FD-C_T282E) in combination with 14-3-3 can bind to all four DNA sequences tested.
323 Furthermore, we detected a supershift for all palindromic sites tested, included the C-
324 box, when we added TFL1. In contrast, for FT an additional shift resembling the pattern
325 obtained with the G-box in *SEP3* promoter was only observed for “site 2” (Fig. 4C,
326 2B). Closer inspection of the nucleotide sequences of the probes used for the G-box in
327 the *SEP3* promoter and the “site 2” in the *API* promoter revealed that the possible FD

328 binding site in the *API* promoter (GTCGAC) is also present in the *SEP3* promoter,
329 where it overlaps with the G-box (Fig. 4D). Interestingly, in the context of the *SEP3*
330 probe, full-length FD and FD-C tolerated mutating the core of the G-box from CG to
331 GC, whereas CG to TA mutations as well as converting the G-box to a C-box
332 (GACGTC) abolished binding (Fig. S4D). To further test if “site 2” on the *API*
333 promoter constitutes a real FD binding site, we mutated its core from CG to TA and
334 checked whether this was sufficient to abolish binding. Results show that indeed the
335 binding of FD to this mutated version of “site 2” was strongly reduced, except in the
336 presence of TFL1 (Fig. S4E).

337 Taken together, our findings exclude the C-box as the FD binding site in the *API*
338 promoter. Furthermore, our results suggest that *in vitro* FD can bind to other motifs
339 besides the G-box, possibly through interaction with partners other than 14-3-3 and
340 FT/TSF, and we characterized possible a new binding site (GTCGAC) that could
341 constitute the true FD binding site in the *API* promoter.

342

343 **Differentially expressed genes at the SAM and direct targets of FD**

344 To test which of the 595 high confidence binding sites we had identified by ChIP-seq
345 at the SAM were in fact transcriptionally regulated by FD we performed RNA-seq on
346 apices from *fd-2* mutants and the *pFD::GFP:FD fd-2* rescue line. 21 day-old SD-grown
347 seedlings were shifted to LD to induce synchronous flowering and apices were
348 harvested on the day of the transfer to LD (T0), as well as 1, 2, 3, and 5 days after the
349 shift (T1, T2, T3, T5) from three independent biological replicates.

350 Differentially expressed (DE) genes were determined for each time point and genes
351 with an adjusted p-value (padj) lower than 0.1 were selected as significantly DE. We
352 identified in total 1759, 583, 2421, 924, and 153 DE genes in T0, T1, T2, T3, and T5,
353 respectively, corresponding to 4189 unique genes (Fig. 5A, Supplemental Data Set 6).

354 PCA analysis showed that the first and second principal components, which explain
355 37% and 21% of the total variance, corresponded to the different time points and
356 genotypes, respectively (Fig. S5A). The best separation between the genotypes in the
357 PCA was observed at T3 and T5, indicating that FD contributes to the transcriptional
358 changes at the SAM mainly after exposure to two long days. This observation is in
359 agreement with the expression profile of FD, which in the *pFD::GFP:FD* rescue line
360 increased after T2 (Fig. S5B). In contrast, FD expression remained low in the *fd-2*
361 mutant, indicating the validity of our experimental approach (Fig. S5B).

362 Next, we intersected the list of genes that were bound by FD at the SAM (572) with the
363 list of DE genes (4189). In total, 135 (23.6%) of the 572 FD-bound genes were
364 significantly DE at the SAM during the transition to flowering at least at one timepoint,
365 indicating that these genes are transcriptionally regulated by FD, which is more than
366 expected by chance (Fig. 5B, C, Supplemental Data Set 7). Among these 135 directly
367 bound and differentially expressed genes we observed several previously known FD-
368 regulated flowering time and floral homeotic genes including *API*, *FUL*, and *SOCI*
369 (Fig. 1F, S6A). In addition, this set of 135 high-confidence FD targets contained also
370 the MADS box gene *SEP3*, the promoter of which is bound by FD and which is down-
371 regulated in *fd-2* mutant (Fig. 1F, S6A). Interestingly, we did not observe binding of
372 FD to any of the other members of *SEPALLATA* gene family in ChIP-seq samples from
373 the SAM, although we did detect FD binding in promoter regions of *SEP1* and *SEP2*,
374 but not *SEP4*, in ChIP-seq from seedlings in which FD had been misexpressed from the
375 *SUC2* promoter. One possible explanation for this is that the ChIP-seq at the SAM
376 apparently worked less efficiently and identified fewer FD targets than in leaves (595
377 vs. 1754), which might result in a larger number of false negatives. In agreement with
378 this interpretation, *SEP1* is down-regulated in the *fd-2* mutant background (Fig. S6),
379 indicating that FD directly or indirectly regulates the expression of *SEP1* at the SAM.
380 Interestingly, we also found FD bound to *TPR2*, a member of the *TOPLESS (TPL)-*
381 *related* gene family. TPL and its family members (*TPR1*, *TPR2*, *TPR3* and *TPR4*) are
382 strong transcriptional co-repressors that interact with other proteins throughout the
383 plant to modulate gene expression (Causier et al., 2012). *TPR2* is down-regulated in the
384 *fd-2* mutant throughout the floral transition from T0 to T5 (Fig. S6), indicating FD
385 might regulate development at the SAM through *TPR2* in a photoperiod-independent
386 manner.

387 Gene Ontology (GO) analysis of these 135 genes that were bound and differentially
388 expressed by FD revealed significant enrichment in several biological process
389 categories (Fig. S7), including “flower development” and “maintenance of
390 inflorescence meristem identity”, as expected for a flowering time regulator such as
391 FD. More surprisingly, however, genes related to the “response to hormone” category
392 were also significantly overrepresented (Supplemental Data Set 8). Among the 27 genes
393 in this category are four genes that are best known for their role in jasmonate signaling
394 (*MYC2*, *JAZ3*, *JAZ6* and *JAZ9*), three genes directly connected to auxin signaling
395 (*ARF18*, *WES1*, and *DFL1*), four genes involved in abscisic acid signaling (*ALDH33II*,
396 *ATGRDPI*, *HAI1* and *PP2CA*), and the flowering-related gene *SOCI*, which is well-

397 known to be regulated by gibberellins (Supplemental Data Set 8). Closer inspection of
398 the expression profiles of these 27 candidate genes revealed that *ARF18* showed a trend
399 similar to *SOC1*, being strongly induced after T2 in Col-0 but not in *fd-2*. The four
400 jasmonate-related genes showed a peculiar expression profile in *fd-2*: an increase from
401 T0 to T1, a decrease in T2, another increase in T3, and decreasing again in T5. Since
402 this peculiar expression profile was observed in three *JAZ* genes, we checked the
403 remaining genes in this family and found that 11 out of 13 displayed a similar pattern
404 (Fig. S6). Furthermore, this profile was also observed in three other genes, *DMR6*, *ESP*
405 and *TOE2*, that have previously been implicated in pathogen resistance and the
406 jasmonate pathway (Fig. S7B). Taken together, these results suggest that FD plays an
407 active role not only in the regulation of flowering time but also functions to connect
408 different hormone signaling pathways.

409

410 **Validation of FD targets**

411 We selected a subset of putative FD direct target genes and determined their expression
412 in early flowering FD overexpression lines (*p35S::FD*) and Col-0. To minimize any
413 bias due to the early flowering of *p35S::FD*, experiments were carried out in vegetative
414 7-day-old LD-grown seedlings. For validation, we selected genes known to play a
415 major role in floral transition, genes that according to Gene Ontology are involved in
416 flowering time and floral development, and other genes that showed a marked
417 differential expression in *fd-2* but for which a role in flowering time regulation had not
418 previously been studied in detail. qRT-PCR assays confirmed that both *SOC1* and *API*
419 were strongly up-regulated in *p35S::FD* (Fig. 6). Although we had only found *SEP3* to
420 be bound by FD in the SAM ChIP-seq analysis, we tested expression of all four
421 *SEPALLATA* genes (*SEP1 – SEP4*) in the *p35S::FD* line. *SEP3* was the only *SEP* gene
422 that was strongly induced in seedlings in response to *FD* overexpression, while *SEP1*
423 showed only moderate induction. In contrast, expression of *SEP2* and *SEP4* did not
424 show differences between *p35S::FD* and Col-0 (Fig. 6). Interestingly, *SEP1*, *SEP2*, and
425 *SEP3* were also bound by FD in PCC-specific ChIP-seq in seedlings and *SEP1* and
426 *SEP3* exhibited strong differential expression in RNA-seq (Fig. S6). *ASI*, which has
427 been demonstrated to be involved in flowering time by regulation of *FT* expression in
428 leaves (Song et al., 2012), did not show significant difference in expression between
429 Col-0 and *p35S::FD*. We also tested two FRIGIDA-like genes, *FRI-like 4a* and *FRI-*
430 *like 4b*, of which *FRI-like 4b* showed a decreased expression in *p35S::FD*. In addition,
431 we also tested two genes, *MYC2* and *AFRI*, which were bound by FD in both the *pSUC2*

432 and *pFD* ChIP-seq experiments, differentially expressed at the SAM, but not
433 differentially bound in *ft-10 tsf-1* mutant, *i.e.* not directly influenced by the presence of
434 FT and TSF, for their contribution to flowering time regulation. *MYC2* showed no
435 differences in expression in *p35S::FD* compared to Col-0, whereas *AFR1* was up-
436 regulated in *p35S::FD* (Fig. 6). To genetically test the role of these two genes in the
437 regulation of flowering we isolated T-DNA insertion lines and determined their
438 flowering time under LD at 23°C. Both *myc2* and *afr1* were significantly early
439 flowering, both as days to flowering and total leaf number, compared to WT (Fig. 7),
440 confirming their role in regulating the floral transition.

441

442

443

444 **DISCUSSION**

445 *FD* was originally identified as a component of the photoperiod-dependent flowering
446 pathway in *A. thaliana* based on the late flowering phenotype of the loss-of-function
447 mutant (Koornneef et al., 1991). *FD*, which encodes a bZIP transcription factor, is
448 expressed at the SAM prior to the floral transition but does not seem to induce flowering
449 on its own. Later, it was demonstrated that *FD* physically interacts with *FT*, the florigen,
450 and that this interaction is important for its function as a promoter of flowering (Abe et
451 al., 2005; Wigge et al., 2005). In addition, *FD* was found to also interact with *TFL1*,
452 which is normally expressed in the SAM and antagonizes the function of *FT* as floral
453 activator. This and other findings led to the hypothesis that *FD* is held in an inactive
454 state in the vegetative SAM through interaction with *TFL1*. When *FT* is induced in the
455 PCCs and transported to the SAM in response to inductive photoperiod, *FT* competes
456 with *TFL1* for interaction with *FD*, eventually resulting in the formation of
457 transcriptionally active *FD-FT* complexes (Ahn et al., 2006). However, the exact
458 molecular mechanisms of *FD* action and its genome-wide targets remained largely
459 unknown. Here we employed biochemical, genomic, and transcriptomic approaches to
460 clarify the role of *FD* in the regulation of flowering transition in *A. thaliana*.

461 We found that neither *FT* nor *TSF* are required for *FD* to bind to DNA but that their
462 presence increases the enrichment of *FD* on a subset of target loci, which encode for
463 known flowering time and floral homeotic genes such as *API*, *SEP1*, *SEP2*, and *FUL*.
464 Our data are compatible with the model described by (Ahn et al., 2006), according to
465 which *FT* acts as a transcriptional coactivator. Without *FT*, *FD* would still be capable
466 of binding to DNA but would not activate transcription. This hypothesis is supported

467 by our finding that FD is capable of binding to DNA by itself *in vitro*. However, we
468 can not exclude the possibility that the binding of FD to DNA we observed in the
469 *pSUC2::GFP:FD ft-10 tsf-1* reporter line could be mediated by the floral repressors
470 BFT and ATC, both of which are expressed in the leaf vasculature and are known to
471 interact with FD (Ryu et al., 2014; Huang et al., 2012; Yoo et al., 2010).

472 In this context, our EMSA results are of particular interest as they demonstrate that, at
473 least *in vitro*, TFL1 is capable of interacting with unphosphorylated FD via 14-3-3
474 proteins, suggesting that the transcriptionally inactive ternary FD/14-3-3/TFL1
475 complex could be the ground state at the SAM. Only after FD has been phosphorylated
476 can FT, together with 14-3-3 proteins, form an active FAC to induce flowering. This
477 requirement for phosphorylation of T282 of FD adds another safeguard to the system
478 that might help to prevent disastrous premature induction of flowering. Our results
479 clearly suggest that phosphorylation is important for FD function and add to our
480 understanding concerning the role of FD phosphorylation, which had mostly been based
481 on the analyses of a FD/14-3-3/Hd3a complex in rice using a short FD peptide (Taoka
482 et al., 2011; Kaneko-Suzuki et al., 2018).

483 Which kinases regulate phosphorylation of FD *in vivo* has been a matter of debate, but
484 recently two calcium-dependent kinases, CPK6 and CPK33, have been shown to
485 phosphorylate FD (Kawamoto et al., 2015). Building on this, we show that expression
486 of a non-phosphorable version of the FD protein (T282A) under the control of the *pFD*
487 promoter failed to rescue the late flowering of *fd-2*. In contrast, expression of a
488 phosphomimic version of FD (T282E) resulted in early flowering when expressed in
489 *fd-2*. Similar results were obtained using a S281E phosphomimic FD. These results
490 indicate that the phosphorylation of FD must be tightly controlled to prevent premature
491 flowering. Interestingly, both CPK6 and CPK33 are more strongly expressed in
492 transition apices than they are in vegetative apices (Schmid et al., 2005), which would
493 be in agreement with an activation of FD by these two kinases during floral induction.
494 Somewhat surprisingly, we observed that the C-terminal part of the FD protein, which
495 includes the bZIP domain and the phosphorylation site, was sufficient to trigger
496 complex formation with FT, TFL1 and 14-3-3 proteins. This suggests that the N-
497 terminal region of FD, which is predicted to be highly unstructured and contains a
498 stretch of 25 amino acids containing 19 serine residues, might be dispensable for
499 FD/14-3-3/FT complex formation. However, the N-terminal region of FD is
500 evolutionarily conserved, indicating that it may contribute to FD function. This notion

501 is supported by our observation that expression of the C-terminal part of FD in plants
502 only partially restored the late flowering of *fd-2* mutants.

503 Part of the flowering promoting activity of FD can probably be expressed through its
504 effect on members of the *SEP* gene family of MADS-domain transcription factors,
505 which are required for the activity of the A-, B-, C-, and D-class floral homeotic genes
506 (reviewed in Theissen et al., 2016). In addition to its function as a floral homeotic gene,
507 *SEP3* has also been reported to promote flowering by accumulation in leaves under FT
508 regulation (Teper-Bamnolker and Samach, 2005) and as downstream target of the
509 miR156-SPL3-FT module in response to ambient temperature (Hwan Lee et al., 2012).
510 However, how *SEP3* is regulated at the SAM has remained unclear. Interestingly, we
511 found that FD bound strongly to the *SEP3* promoter and *SEP3* is downregulated in the
512 *fd-2* mutant. As FD also binds to the promoter and activated expression of the A-class
513 gene *API*, FD activity might be sufficient to induce formation of sepals, which form
514 the outmost floral whorl, and which according to the quartet model require the
515 formation of a SEP/AP1 complex (Theissen et al., 2016). However, it should be noted
516 that *fd* mutants do not display notable homeotic defects, indicating that FD is clearly
517 not the only factor regulating *SEP3* and *API* expression. Furthermore, binding of FD
518 to *API* is unlikely to be mediated by a C-box as previously suggested (Wigge et al.,
519 2005; Taoka et al., 2011) as the summits of the ChIP-seq peaks do not cover this region
520 of the *API* promoter. Interestingly, this region contains several palindromic sequences,
521 one or more of which most likely mediate FD binding to the *API* promoter.

522 Another interesting outcome of our analyses is the indication that FD might contribute
523 to the regulation of other processes in the plant besides flowering. In particular, we
524 found that FD directly regulated the expression of genes involved in several hormone
525 signaling pathways. For example, we observed FD binding to the promoter of *MYC2*, a
526 bHLH transcription factor that plays a key role in jasmonate response. It has been
527 shown that MYC2 forms a complex with JAZ proteins and the TPL co-repressor, and
528 that this interaction is dependent on NINJA proteins (Pauwels et al., 2010). In this
529 context it is noteworthy that FD also bound directly to the promoter of *TPR2* promoter
530 and that *TPR2* was strongly downregulated in *fd-2*. This finding indicates that FD not
531 only regulates MYC2 but also at least some of the interacting TPL-like transcriptional
532 co-repressors. Finally, we also observed strong binding of FD to (and misexpression
533 of) a number of JAZ genes in either PCCs and/or the SAM in our ChIP-seq and RNA-
534 seq data. Taken together, this indicates that FD may control the expression of three core
535 components of jasmonate signaling: *MYC2*, *TPR2*, and several *JAZ* genes. These results

536 support earlier findings that had reported a link between jasmonate signaling
537 components and flowering time regulation. JAZ proteins have been shown to regulate
538 flowering in leaves through the direct interaction with the floral repressors TOE1 and
539 TOE2, which is also bound by FD and differentially expressed in *fd-2*, and the
540 regulation of FLC that negatively regulate *FT* expression (Zhai et al., 2015). Moreover,
541 MYC2 has also been reported to affect flowering time by regulating *FT* expression in
542 leaves (Zhai et al., 2015; Wang et al., 2017). However, previous publications had
543 reported contradictory results concerning the flowering phenotype of the *myc2* mutant,
544 ranging from late flowering (Gangappa and Chattopadhyay, 2010) to early flowering
545 (Wang et al., 2009) or no obvious effect (Major et al., 2017). In our conditions the *myc2*
546 mutant exhibited early flowering compared to Col-0, in agreement with the report from
547 Wang and colleagues (Wang et al., 2009) (Fig. 7). We also identified *ARF18*, a member
548 of the auxin response factor family, as a direct target of FD. Notably, the expression of
549 *ARF18* is strongly induced after T2 in Col-0 but not in *fd-2* and this pattern is the same
550 of known direct FD targets, e.g.: *API* and *SOC1*. Moreover, *ARF18* is also induced at
551 the SAM during the floral transition (Schmid et al., 2005) providing further evidence
552 for a possible link between FD and *ARF18*. In summary, our findings suggest a link
553 between the photoperiodic pathway gene FD and hormone signaling pathways.
554 Although further experiments will be necessary to better understand this connection,
555 we hypothesize that linking hormone signaling to flowering time through FD regulation
556 might allow plants to fine tune their flowering time response to abiotic and biotic
557 stresses.

558 Apart from connecting FD with hormone signaling we characterized another target gene
559 in more detail, *AFRI*. This gene encodes a putative histone deacetylase subunit and had
560 previously been shown to negatively affect the expression of *FT* in the leaves. Further,
561 *afr1* mutations cause early flowering (Fig. 7)(Gu et al., 2013). Our results suggest that
562 FD might modulate flowering through ARF1-mediated regulation of chromatin.
563 However, such regulation would most likely not be mediated by *FT*, as *FT* is normally
564 not expressed at the SAM.

565 Taken together, our results support the role of FD as a key regulator of photoperiod-
566 induced flowering and the expression of A- and E-class floral homeotic genes in *A.*
567 *thaliana*. Furthermore, FD might play an important role in coordinating the crosstalk
568 between the photoperiod pathway and hormone signaling pathways and provide a
569 convergence point for diverse environmental and endogenous signaling pathways.

570

571

572

573 **MATERIAL AND METHODS**

574 **Plant materials and growth conditions**

575 *Arabidopsis thaliana* accession Col-0 was used as wild-type. Mutants investigated in
576 this study are: *fd-2* (SALK_013288), *ft-10* (GABI_290E08), *tsf-1* (SALK_087522),
577 *myc2* (SALK_017005), *arf1* (SALK_026979) (Tab. S1). Seeds were stratified for 3
578 days in 0.1% agar in the dark at 4°C and directly planted on soil. Plants were grown on
579 soil under long days (16 hours of light and 8 hours of night) or under short days (8 hours
580 of light and 16 hours of night) at 23°C and 65% relative humidity. Plants used for
581 flowering time measurements were grown in a randomized design to reduce location
582 effects in the growth chambers.

583

584 **DNA vectors and plant transformation**

585 DNA vectors used in this study are listed in table S2. Coding sequences were amplified
586 by PCR from cDNA and cloned into either pGREEN-IIS vectors for flowering time
587 studies or pET-M11 vectors for protein expression. Final constructs were transformed
588 by electroporation in *Agrobacterium tumefaciens* and *Arabidopsis* plants of accession
589 Col-0 and *fd-2* were transformed by the floral dip method. Basta treatment (0.1% v/v)
590 was used for screening for transgenic lines.

591

592 **ChIP and ChIP-seq**

593 Approximately 1.5 grams of seedlings (*pSUC2::GFP:FD* and *pSUC2::GFP:NLS* in
594 both Col-0 and *ft-10 tsf-1*) or 300 mg of manually dissected apices (*pFD::GFP:FD* in
595 *fd-2*; Col-0) from 16 day old plants grown on soil under long day 23°C were harvested
596 and fixed in 1% formaldehyde under vacuum for 1 hour. ChIP was performed as
597 previously described (Kaufmann et al., 2010) with the following minor changes:
598 sonication was performed using a Covaris E220 system (conditions: intensity 200 W,
599 duty 20, cycles 200, time 120 seconds), incubation time with antibody was increased to
600 over-night, incubation time with protein-A agarose beads was increased to 4 hours,
601 purification of DNA after de-cross linking was performed with MinElute Reaction
602 Cleanup Kit (Qiagen).

603 Anti-GFP from AbCam (ab290) was used for immuno-precipitation. ChIP-seq libraries
604 were prepared using TruSeq ChIP Library Preparation Kit (Illumina) and BluePippin
605 was used for gel size selection of fragments between 200 bp and 500 bp. Final

606 concentration and size distribution of the libraries were tested with Qubit and
607 BioAnalyzer (Agilent High Sensitivity DNA Kit). Libraries were sequenced on an
608 Illumina HiSeq3000 system using the 50bp single end kit.

609

610 **RNA extraction, RNA-seq and expression analysis**

611 For RNA-seq, Col-0 and *fd-2* plants were grown for 21 days under short days at 23°C
612 and then shifted to long days 23°C. RNA was extracted from manually dissected apices
613 collected the day of the shift (T0) and 1, 2, 3, 5 days after shifting (T1, T2, T3 and T5
614 respectively) using the RNeasy Plant Kit (Qiagen) according to the manufacturer's
615 instructions. RNA integrity and quantification were determined on a BioAnalyzer
616 system. 1 µg of RNA was used to prepare libraries using the TruSeq RNA Library
617 Prep Kit (Illumina). All libraries were quality controlled and quantified by Qubit and
618 Bioanalyzer and run on a Illumina HiSeq3000 with 50bp single end kit.

619 Validation of the selected FD targets was performed in 7 day old seedlings grown on
620 soil under long days at 23°C.

621 RNA was extracted using the RNeasy Plant Kit (Qiagen) according to the
622 manufacturer's instructions. cDNA was synthesized using the RevertAid RT Reverse
623 Transcription Kit (ThermoScientific) according to the manufacturer's instructions.
624 qRT-PCRs were performed on a CFX96 Touch Real-time PCR Detection System
625 (BioRad) using LightCycler 480 SYBR Green I Master (Roche). Oligonucleotides used
626 as primers for qRT-PCR are listed in table S3.

627

628 **ChIP-seq and RNA-seq analysis**

629 Raw data from ChIP-seq were trimmed of adapters and aligned to the *A. thaliana*
630 genome (TAIR10 release) using bwa (Li and Durbin, 2010). MACS2 was used to call
631 peaks using default parameters (Zhang et al., 2008). Mapped reads from samples
632 expressing GFP:NLS under the same promoter of the GFP:FD (*e.g.*: *pSUC2*) in
633 seedlings experiments or Col-0 without any vector in apices experiments were used for
634 normalization. Differentially bound analyses were carried out using the R package
635 "DiffBind" using default parameters (Stark, 2011; Ross-Innes et al., 2012).

636 For the analysis of RNA-seq data, sequencing reads mapping to rRNAs were filtered
637 out using Sortmerna (Kopylova et al., 2012) and the remaining reads were trimmed of
638 adapters using Trimmomatic (Bolger et al., 2014). Alignment to the *A. thaliana* genome
639 was performed with STAR (Dobin et al., 2013) and read counted with HTSeqCount

640 (Anders et al., 2015). Differential expression analysis was performed using DESeq2
641 with default parameters (Love et al., 2014).

642

643 **Electrophoretic Mobility Shift Assays (EMSA)**

644 Coding sequences of both the wild-type version as well as the phosphomimic variant
645 (T282) of *FD* and its C-terminal domain (*FD-C*, amino acids: 203-285), *14-3-3v*
646 (At3g02520; *GRF7*), *FT*, and *TFL1* were amplified by PCR to generate N-terminal 6X-
647 His-tag CDS which were cloned into pETM-11 expression vector by restriction enzyme
648 cloning. All plasmids were transformed into *Escherichia coli* strain Rosetta plysS and
649 proteins were induced with 1mM IPTG at 37°C over-night. Cell lysis was performed
650 by sonication and proteins were purified using His60 columns (Clontech) and eluted in
651 50 mM of sodium phosphate buffer pH 8.0, 300 mM NaCl, 300 mM Imidazole. EMSA
652 was performed using 5'-Cy3-labeled, double-stranded oligos of 30 bp covering the G-
653 box contained in the *SEP3* promoter as a probe (Eurofins). For probe synthesis, single
654 strand oligos were annealed in annealing buffer (10 mM Tris pH 8.0, 50 mM NaCl, 1
655 mM EDTA pH 8.0). Binding reactions were carried out in buffer containing 10 mM
656 Tris pH 8.0, 50 mM NaCl, 10 μM ZnSO₄, 50 mM KCl, 2.5% glycerol, 0.05% NP-40 in
657 a total volume of 20 μl. The binding reaction was kept in dark at room temperature for
658 20 minutes and then loaded in native 8% polyacrylamide gel and run in 0.5X TBE at
659 4°C in dark. Results were visualized using a Typhoon imaging system.

660

661

662

663 **ACCESSION NUMBERS**

664 RNA-seq and ChIP-seq data have been deposited at European Nucleotide Archive
665 (ENA) under accession number PRJEB24873 and PRJEB24874, respectively.

666

667

668

669 **SUPPLEMENTARY MATERIAL**

670 **Supplemental Figures**

671 **Figure S1.** ChIP-seq summary statistics for the different biological replicates:

672 *pSUC2::GFP:FD* in Col-0 (A, D, G, J) and *ft-10 tsf-1* mutant background (B,
673 E, H, K), *pFD::GFP:FD* in *fd-2* mutant background (C, F, I, L).

674 **Figure S2.** Verification of comparability of controls used for normalization of FD
675 (*pSUC2::GFP:FD*) ChIP-seq in WT and *ft-10 tsf-1* seedlings.

676 **Figure S3.** Effect of misexpression of FD on gene expression and flowering time.

677 **Figure S4.** Electrophoretic mobility shift assays (EMSAs) to test FD binding to the
678 *SEP3* and *API* promoters.

679 **Figure S5.** Summary of RNA-seq results.

680 **Figure S6.** Expression profile of selected FD target genes.

681 **Figure S7.** Gene Ontology (GO) analysis on the subset of 135 direct genes of FD.

682

683 **Supplemental Tables**

684 **Table S1.** List of mutants and oligos for genotyping used in the study.

685 **Table S2.** List of vectors used in the study.

686 **Table S3.** List of oligos used for qRT-PCR in the study.

687

688 **Supplemental Data Sets**

689 **Supplemental Data Set 1.** List of 1754 FD-bound peaks identified in seedlings
690 expressing *pSUC2::GFP:FD* in Col-0.

691 **Supplemental Data Set 2.** List of 2427 FD-bound peaks identified in seedlings
692 expressing *pSUC2::GFP:FD* in *ft-10 tsf-1*.

693 **Supplemental Data Set 3.** List of 1514 FD-bound peaks detected in seedlings
694 expressing *pSUC2::GFP:FD* in either Col-0 or *ft-10 tsf-1*.

695 **Supplemental Data Set 4.** List of 917 peaks that were differential bound in
696 seedlings expressing *pSUC2::GFP:FD* in either Col-0 or *ft-10 tsf-1*.

697 **Supplemental Data Set 5.** List of 595 shared FD-bound peaks in apices
698 *pFD::GFP:FD fd-2* rescue line.

699 **Supplemental Data Set 6.** List of differentially expressed genes.

700 **Supplemental Data Set 7.** List of 135 potential direct targets of FD.

701 **Supplemental Data Set 8.** List of 27 genes related to "response to hormone"
702 category within the subset of the 135 direct target of FD.

703

704

705

706 **ACKNOWLEDGEMENTS**

707 We thank Diana Saez for help in isolating homozygous *myc2* and *afr1* mutants, the
708 Protein Expertise Platform (PEP) at the Chemical Biological Center (KBC) at Umeå

709 University for help with protein purification, and Nicolas Delhomme from the UPSC
710 Bioinformatics Facility for assistance with submission of sequencing data. We
711 acknowledge funding to the UPSC through grants from VINNOVA and The Knut and
712 Alice Wallenberg Foundation. S.C. was supported through a Humboldt Foundation
713 long-term postdoctoral fellowship. L.Y. acknowledges funding from the European
714 Research Council (ERC) under the European Union's Horizon 2020 research and
715 innovation programme (grant agreement 679056) and the UK Biological and
716 Biotechnology Research Council (BBSRC) via grant BB/P013511/1 to the John Innes
717 Centre. Supported through the Sonderforschungsbereich 1101 (Collaborative Research
718 Centre 1101), project grant SFB1101/1-B04, and a research project grant from the Knut
719 and Alice Wallenberg Foundation (2016.0025) to M.S.

720

721

722

723 **FIGURE LEGENDS**

724 **Figure 1.** Identification of FD targets by *pSUC2::GFP:FD* ChIP-seq in Col-0 and *ft-*
725 *10 tsf-1* and *pFD::GFP:FD* ChIPseq in *fd-2*.

726 (A) Annotation of high-confidence peaks found in two biological replicates in Col-
727 0 and *ft-10 tsf-1*.

728 (B) 4-set venn diagram representing the overlapping peaks among all the biological
729 replicates from Col-0 and *ft-10 tsf-1*. The majority of the peaks (1514) are
730 shared between the two genetic backgrounds.

731 (C) Nucleotide logo of the predicted FD binding site.

732 (D) Correlation heatmap calculated on a binding matrix based on ChIP-seq reads
733 counts for Col-0 and *ft-10 tsf-1* samples (affinity scores). The presence/absence
734 of FT and TSF is sufficient to discriminate the two genetic backgrounds.

735 (E) Differentially bound (DB) peaks between Col-0 and *ft-10 tsf-1*. Red dots
736 indicate differentially bound peaks with a FDR < 0.05.

737 (F) Reads from Col-0, *ft-10 tsf-1* and control sample mapped against selected
738 flowering related genes.

739 (G) Annotation of high-confidence peaks identified by ChIPseq in two biological
740 replicates in *pFD::GFP:FD fd-2*.

741 (H) Nucleotide logo of the predicted FD binding site at the SAM.

742

743 **Figure 2.** The C-terminal part of FD (FD-C) binds to a G-box in the *SEP3* promoter in
744 vitro.

745 (A) Electrophoretic mobility shift assay (EMSA) of the wild-type form of FD-C in
746 combination with 14-3-3v, FT, and TFL1. FD-C weakly binds the probe on its
747 own but it is not able to form a complex with 14-3-3v and FT. However, FD-C
748 forms a complex with 14-3-3v and TFL1 capable of binding the G-box.

749 (B) Phosphomimic version of FD-C (FD-C_T282E) in combinations with 14-3-3v,
750 FT and TFL1. The phosphomimic version of FD-C binds the G-box alone and
751 interacts with 14-3-3v, which facilitates interaction with FT and TFL1. Both
752 wild-type and phosphomimic version of FD-C require 14-3-3v for interaction
753 with FT or TFL1.

754 Asterisk (*) indicate shifted probe.

755

756 **Figure 3.** Phosphorylation of FD at threonine 282 (T282) modulates flowering time in
757 *A. thaliana*.

758 Expression of wildtype (WT) *pFD::FD* rescues the late flowering phenotype of
759 *fd-2*. Mutation of T282 to alanine (T>A) in *pFD::FD_T282A*, which prevents
760 phosphorylation, abolishes rescue of *fd-2*. Mutations mimicking constitutive
761 phosphorylation of T282 (T>E), S281 (S>E), or both (ST>EE) induce early
762 flowering. Results are shown for two independent homozygous lines per
763 construct. Statistical significance was calculated using an unpaired t-test
764 compared to Col-0. *** indicates a significance level $p < 0.01$.

765

766 **Figure 4.** Mapping of the FD binding site in the *API* promoter.

767 (A) Normalized reads from six ChIP-seq experiments mapped on the *API* locus. The
768 result shows that the C-box is upstream of all peak summits.

769 (B) Nucleotide sequence encompassing the six peak summits shows several
770 palindromic regions representing putative binding sites of *FD* on *API* promoter.
771 The distance between the closest potential FD binding site under the ChIP-seq
772 peaks and the C-box is 92 bp. Black triangles indicate the summits of the six
773 separate ChIP-seq experiments. Putative FD binding sites are underlined and
774 numbered from 1 to 4.

775 (C) Electrophoretic mobility shift assay (EMSA) of the phosphomimic version of
776 FD-C (FD-C_T282E) in combinations with 14-3-3v, FT and TFL1 using the
777 four putative binding sites reported in panel B. Free probes are not visible

778 because gels were running longer to maximize the distance between shifted
779 probes. Coloured squares indicate shifted probes.

780 **(D)** Comparison of the probes used for EMSA: the G-box in *SEP3* promoter (Fig. 2)
781 and the binding site 2 in *API* promoter. The putative FD binding site in *API*
782 promoter is also conserved in *SEP3* promoter and overlaps with the G-box.

783

784 **Figure 5.** RNA-seq results at the shoot apical meristem.

785 **(A)** Scatter blot of differentially expressed (DE) genes between the *fd-2* mutant and
786 *pFD::GFP-FD fd-2* (control) at 5 time points before and during the transition
787 to photoperiod-induced flowering. T0 – T5 indicate day of sample collection
788 before (T0) and 1, 2, 3, 5 days after shifting plants to long day. Red dots
789 indicate DE genes with a $p_{adj} < 0.1$.

790 **(B)** Venn diagrams showing the overlap between FD target genes identified by
791 ChIP-seq and DE genes found by RNA-seq at the SAM at each time point.

792 **(C)** Venn diagram showing the overlap between FD target unique genes identified
793 by ChIP-seq and DE unique genes in at least one time point found by RNA-
794 seq at the SAM. A total of 135 genes were classified as putative direct targets
795 of FD. Statistical significance was calculated using the Fisher's exact test.
796 Asterisk (*) indicates a significance level $p = 1.03E-07$.

797

798 **Figure 6.** Validation of FD targets in Col-0 and *p35S::FD*.

799 qRT-PCR analysis of 12 putative direct targets of FD. RNA was isolated from
800 7 day old seedlings to minimize any bias due to the early flowering of the
801 *p35S::FD* line. Error bars represent \pm SD from three biological replicates.

802

803 **Figure 7.** Flowering time of *myc2* and *afr1*.

804 Flowering time of homozygous of *myc2* and *afr1* T-DNA insertion lines was
805 scored as days to flowering (A) and total leaves (B). Statistical significance
806 was calculated using unpaired t-test compared to Col-0. *** and ** indicate a
807 significance level $p < 0.01$ and $p < 0.05$, respectively.

808

809 REFERENCES

- 810 **Abe M, Kobayashi Y, Yamamoto S, Daimon Y, Yamaguchi A, Ikeda Y, Ichiniki**
 811 **H, Notaguchi M, Goto K, Araki T** (2005) FD, a bZIP protein mediating
 812 signals from the floral pathway integrator FT at the shoot apex. *Science*
 813 **309**: 1052-1056
- 814 **Ahn JH, Miller D, Winter VJ, Banfield MJ, Lee JH, Yoo SJ, Henz SR, Brady RL,**
 815 **Weigel D** (2006) A divergent external loop confers antagonistic activity
 816 on floral regulators FT and TFL1. *EMBO J* **25**: 605-614
- 817 **An H, Roussot C, Suarez-Lopez P, Corbesier L, Vincent C, Pineiro M,**
 818 **Hepworth S, Mouradov A, Justin S, Turnbull C, Coupland G** (2004)
 819 CONSTANS acts in the phloem to regulate a systemic signal that induces
 820 photoperiodic flowering of Arabidopsis. *Development* **131**: 3615-3626
- 821 **Anders S, Pyl PT, Huber W** (2015) HTSeq--a Python framework to work with
 822 high-throughput sequencing data. *Bioinformatics* **31**: 166-169
- 823 **Benlloch R, Kim MC, Sayou C, Thevenon E, Parcy F, Nilsson O** (2011)
 824 Integrating long-day flowering signals: a LEAFY binding site is essential
 825 for proper photoperiodic activation of APETALA1. *Plant J* **67**: 1094-1102
- 826 **Bolger AM, Lohse M, Usadel B** (2014) Trimmomatic: a flexible trimmer for
 827 Illumina sequence data. *Bioinformatics* **30**: 2114-2120
- 828 **Causier B, Ashworth M, Guo W, Davies B** (2012) The TOPLESS interactome: a
 829 framework for gene repression in Arabidopsis. *Plant Physiol* **158**: 423-
 830 438
- 831 **Corbesier L, Vincent C, Jang S, Fornara F, Fan Q, Searle I, Giakountis A,**
 832 **Farrona S, Gissot L, Turnbull C, Coupland G** (2007) FT Protein
 833 Movement Contributes to Long-Distance Signaling in Floral Induction of
 834 Arabidopsis. *Science* **316**: 1030-1033
- 835 **Deeken R, Ache P, Kajahn I, Klinkenberg J, Bringmann GRH** (2008)
 836 Identification of Arabidopsis thaliana phloem RNAs provides a search
 837 criterion for phloem-based transcripts hidden in complex datasets of
 838 microarray experiments. *Plant J* **55**: 746-759
- 839 **Dobin A, Davis CA, Schlesinger F, Drenkow J, Zaleski C, Jha S, Batut P,**
 840 **Chaisson M, Gingeras TR** (2013) STAR: ultrafast universal RNA-seq
 841 aligner. *Bioinformatics* **29**: 15-21
- 842 **Gangappa SN, Chattopadhyay S** (2010) MYC2, a bHLH transcription factor,
 843 modulates the adult phenotype of SPA1. *Plant Signal Behav* **5**: 1650-1652
- 844 **Gu X, Wang Y, He Y** (2013) Photoperiodic regulation of flowering time through
 845 periodic histone deacetylation of the florigen gene FT. *PLoS Biol* **11**:
 846 e1001649
- 847 **Hanano S, Goto K** (2011) Arabidopsis TERMINAL FLOWER1 is involved in the
 848 regulation of flowering time and inflorescence development through
 849 transcriptional repression. *Plant Cell* **23**: 3172-3184
- 850 **Hanzawa Y, Money T, Bradley D** (2005) A single amino acid converts a
 851 repressor to an activator of flowering. *Proc Natl Acad Sci USA* **102**: 7748-
 852 7753
- 853 **Ho WW, Weigel D** (2014) Structural Features Determining Flower-Promoting
 854 Activity of Arabidopsis FLOWERING LOCUS T. *Plant Cell* **26**: 552-564
- 855 **Huang NC, Jane WN, Chen J, Yu TS** (2012) Arabidopsis thaliana
 856 CENTRORADIALIS homologue (ATC) acts systemically to inhibit floral
 857 initiation in Arabidopsis. *Plant J* **72**: 175-184

858 **Hwan Lee J, Joon Kim J, Ahn JH** (2012) Role of SEPALLATA3 (SEP3) as a
859 downstream gene of miR156-SPL3-FT circuitry in ambient temperature-
860 responsive flowering. *Plant Signal Behav* **7**: 1151-1154

861 **Jakoby M, Weisshaar B, Dröge-Laser W, Vicente-Carbajosa J, Tiedemann J,**
862 **Kroj T, Parcy F** (2002) bZIP transcription factors in Arabidopsis. *Trends*
863 *Plant Sci* **7**: 106-111

864 **Jung JH, Ju Y, Seo PJ, Lee JH, Park CM** (2012) The SOC1-SPL module integrates
865 photoperiod and gibberellic acid signals to control flowering time in
866 Arabidopsis. *Plant J* **69**: 577-588

867 **Kaneko-Suzuki M, Kurihara-Ishikawa R, Okushita-Terakawa C, Kojima C,**
868 **Nagano-Fujiwara M, Ohki I, Tsuji H, Shimamoto K, Taoka K** (2018)
869 TFL1-Like Proteins in Rice Antagonize Rice FT-Like Protein in
870 Inflorescence Development by Competition for Complex Formation with
871 14-3-3 and FD. *In, Vol 59. Plant Cell Physiol*, pp 458-468

872 **Kaufmann K, Muino JM, Osteras M, Farinelli L, Krajewski P, Angenent GC**
873 (2010) Chromatin immunoprecipitation (ChIP) of plant transcription
874 factors followed by sequencing (ChIP-SEQ) or hybridization to whole
875 genome arrays (ChIP-CHIP). *Nat Protoc* **5**: 457-472

876 **Kawamoto N, Sasabe M, Endo M, Machida Y, Araki T** (2015) Calcium-
877 dependent protein kinases responsible for the phosphorylation of a bZIP
878 transcription factor FD crucial for the florigen complex formation. *Sci Rep*
879 **5**: 8341

880 **Kim W, Park TI, Yoo SJ, Jun AR, Ahn JH** (2013) Generation and analysis of a
881 complete mutant set for the Arabidopsis FT/TFL1 family shows specific
882 effects on thermo-sensitive flowering regulation. *J Exp Bot* **64**:1715-1729

883 **Koornneef M, Hanhart CJ, van der Veen JH** (1991) A genetic and physiological
884 analysis of late flowering mutants in Arabidopsis thaliana. *Mol Gen Genet*
885 **229**: 57-66

886 **Kopylova E, Noe L, Touzet H** (2012) SortMeRNA: fast and accurate filtering of
887 ribosomal RNAs in metatranscriptomic data. *Bioinformatics* **28**: 3211-
888 3217

889 **Lee J, Lee I** (2010) Regulation and function of SOC1, a flowering pathway
890 integrator. *J Exp Bot* **61**: 2247-2254

891 **Li H, Durbin R** (2010) Fast and accurate long-read alignment with Burrows-
892 Wheeler transform. *Bioinformatics* **26**: 589-595

893 **Love MI, Huber W, Anders S** (2014) Moderated estimation of fold change and
894 dispersion for RNA-seq data with DESeq2. *Genome Biol* **15**: 550

895 **Machanick P, Bailey TL** (2011) MEME-ChIP: motif analysis of large DNA
896 datasets. *Bioinformatics* **27**: 1696-1697

897 **Major IT, Yoshida Y, Campos ML, Kapali G, Xin XF, Sugimoto K, de Oliveira**
898 **Ferreira D, He SY, Howe GA** (2017) Regulation of growth-defense
899 balance by the JASMONATE ZIM-DOMAIN (JAZ)-MYC transcriptional
900 module. *New Phytol* **215**: 1533-1547

901 **Mathieu J, Warthmann N, Kuttner F, Schmid M** (2007) Export of FT protein
902 from phloem companion cells is sufficient for floral induction in
903 Arabidopsis. *Curr Biol* **17**: 1055-1060

904 **Moon J, Lee H, Kim M, Lee I** (2005) Analysis of flowering pathway integrators in
905 Arabidopsis. *Plant Cell Physiol* **46**: 292-299

906 **Moon J, Suh S-S, Lee H, Choi K-R, Hong CB, Paek N-C, Kim S-G, Lee I** (2003)
907 TheSOC1MADS-box gene integrates vernalization and gibberellin signals
908 for flowering in Arabidopsis. *Plant J* **35**: 613-623

909 **Pauwels L, Barbero GF, Geerinck J, Tilleman S, Grunewald W, Perez AC,**
910 **Chico JM, Bossche RV, Sewell J, Gil E, Garcia-Casado G, Witters E, Inze**
911 **D, Long JA, De Jaeger G, Solano R, Goossens A** (2010) NINJA connects
912 the co-repressor TOPLESS to jasmonate signalling. *Nature* **464**: 788-791

913 **Romera-Branchat M, Andres F, Coupland G** (2014) Flowering responses to
914 seasonal cues: what's new? *Curr Opin Plant Biol* **21**: 120-127

915 **Ross-Innes CS, Stark R, Teschendorff AE, Holmes KA, Ali HR, Dunning MJ,**
916 **Brown GD, Gojis O, Ellis IO, Green AR, Ali S, Chin SF, Palmieri C,**
917 **Caldas C, Carroll JS** (2012) Differential oestrogen receptor binding is
918 associated with clinical outcome in breast cancer. *Nature* **481**: 389-393

919 **Ryu JY, Lee HJ, Seo PJ, Jung JH, Ahn JH, Park CM** (2014) The Arabidopsis floral
920 repressor BFT delays flowering by competing with FT for FD binding
921 under high salinity. *Mol Plant* **7**: 377-387

922 **Schmid M, Davison TS, Henz SR, Pape UJ, Demar M, Vingron M, Scholkopf B,**
923 **Weigel D, Lohmann JU** (2005) A gene expression map of Arabidopsis
924 thaliana development. *Nature Gen* **37**: 501-506

925 **Song YH, Lee I, Lee SY, Imaizumi T, Hong JC** (2012) CONSTANS and
926 ASYMMETRIC LEAVES 1 complex is involved in the induction of
927 FLOWERING LOCUS T in photoperiodic flowering in Arabidopsis. *Plant J*
928 **69**: 332-342

929 **Song YH, Shim JS, Kinmonth-Schultz HA, Imaizumi T** (2015) Photoperiodic
930 flowering: time measurement mechanisms in leaves. *Annu Rev Plant Biol*
931 **66**: 441-464

932 **Srikanth A, Schmid M** (2011) Regulation of flowering time: all roads lead to
933 Rome. *Cell Mol Life Sci* **68**: 2013-2037

934 **Stark RBG** (2011) DiffBind: differential binding analysis of ChIP-Seq peak data.
935 [http://bioconductor.org/packages/release/bioc/vignettes/DiffBind/inst/doc/Diff](http://bioconductor.org/packages/release/bioc/vignettes/DiffBind/inst/doc/DiffBind.pdf)
936 [Bind.pdf](http://bioconductor.org/packages/release/bioc/vignettes/DiffBind/inst/doc/DiffBind.pdf)

937 **Taoka K, Ohki I, Tsuji H, Furuita K, Hayashi K, Yanase T, Yamaguchi M,**
938 **Nakashima C, Purwestri YA, Tamaki S, Ogaki Y, Shimada C, Nakagawa**
939 **A, Kojima C, Shimamoto K** (2011) 14-3-3 proteins act as intracellular
940 receptors for rice Hd3a florigen. *Nature* **476**: 332-335

941 **Teper-Bamnolker P, Samach A** (2005) The flowering integrator FT regulates
942 SEPALLATA3 and FRUITFULL accumulation in Arabidopsis leaves. *Plant*
943 *Cell* **17**: 2661-2675

944 **Theissen G, Melzer R, Rumpler F** (2016) MADS-domain transcription factors
945 and the floral quartet model of flower development: linking plant
946 development and evolution. *Development* **143**: 3259-3271

947 **Wang H, Li Y, Pan J, Lou D, Hu Y, Yu D** (2017) The bHLH Transcription Factors
948 MYC2, MYC3, and MYC4 Are Required for Jasmonate-Mediated Inhibition
949 of Flowering in Arabidopsis. *Mol Plant* **10**: 1461-1464

950 **Wang JW, Czech B, Weigel D** (2009) miR156-regulated SPL transcription
951 factors define an endogenous flowering pathway in Arabidopsis thaliana.
952 *Cell* **138**: 738-749

953 **Wigge PA, Chul Kim M, Jaeger KE, Busch W, Schmid M, Lohmann JU, Weigel**
954 **D** (2005) Integration of spatial and temporal information during floral
955 induction in Arabidopsis. *Science* **309**: 1056-1059
956 **Yamaguchi A, Kobayashi Y, Goto K, Abe M, Araki T** (2005) TWIN SISTER OF
957 FT (TSF) acts as a floral pathway integrator redundantly with FT. *Plant*
958 *Cell Physiol* **46**: 1175-1189
959 **Yoo SJ, Chung KS, Jung SH, Yoo SY, Lee JS, Ahn JH** (2010) BROTHER OF FT AND
960 TFL1 (BFT) has TFL1-activity and functions redundantly with TFL1 in
961 inflorescence meristem development in Arabidopsis. *Plant J* **63**: 241-253
962 **Yoo SK, Chung KS, Kim J, Lee JH, Hong SM, Yoo SJ, Yoo SY, Lee JS, Ahn JH**
963 (2005) CONSTANS activates SUPPRESSOR OF OVEREXPRESSION OF
964 CONSTANS 1 through FLOWERING LOCUS T to promote flowering in
965 Arabidopsis. *Plant Physiol* **139**: 770-778
966 **Zhai Q, Zhang X, Wu F, Feng H, Deng L, Xu L, Zhang M, Wang Q, Li C** (2015)
967 Transcriptional Mechanism of Jasmonate Receptor CO11-Mediated Delay
968 of Flowering Time in Arabidopsis. *Plant Cell* **27**: 2814-2828
969 **Zhang Y, Liu T, Meyer CA, Eeckhoutte J, Johnson DS, Bernstein BE, Nusbaum**
970 **C, Myers RM, Brown M, Li W, Liu XS** (2008) Model-based analysis of
971 ChIP-Seq (MACS). *Genome Biol* **9**: R137
972

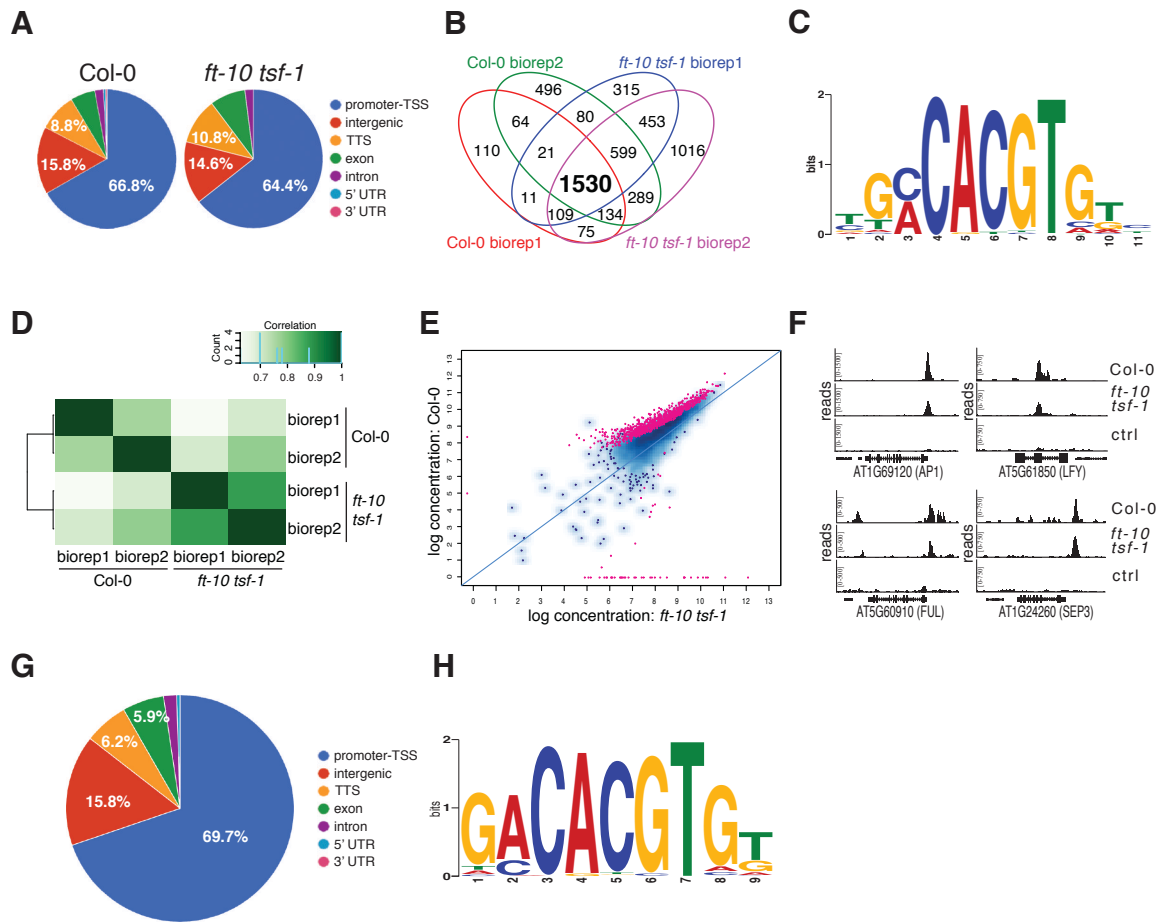


Figure 1. Identification of FD targets by *pSUC2::GFP:FD* ChIP-seq in Col-0 and *ft-10 tsf-1* and *pFD::GFP:FD* ChIPseq in *fd-2*.

- (A) Annotation of high-confidence peaks found in two biological replicates in Col-0 and *ft-10 tsf-1*. TSS: transcription start site; TTS: transcription terminator site.
- (B) 4-set venn diagram representing the overlapping peaks among all the biological replicates from Col-0 and *ft-10 tsf-1*. The majority of the peaks (1530) are shared between the two genetic backgrounds.
- (C) Nucleotide logo of the predicted FD binding site.
- (D) Correlation heatmap calculated on a binding matrix based on ChIP-seq reads counts for Col-0 and *ft-10 tsf-1* samples (affinity scores). The presence/absence of FT and TSF is sufficient to discriminate the two genetic backgrounds.
- (E) Differentially bound (DB) peaks between Col-0 and *ft-10 tsf-1*. Red dots indicate differentially bound peaks with a FDR < 0.05. Blue dots represent peaks that were not significantly differentially bound.
- (F) Reads from Col-0, *ft-10 tsf-1* and control (ctrl) sample mapped against selected flowering-related genes.
- (G) Annotation of high-confidence peaks identified by ChIPseq in two biological replicates in *pFD::GFP:FD fd-2*.
- (H) Nucleotide logo of the predicted FD binding site at the SAM.

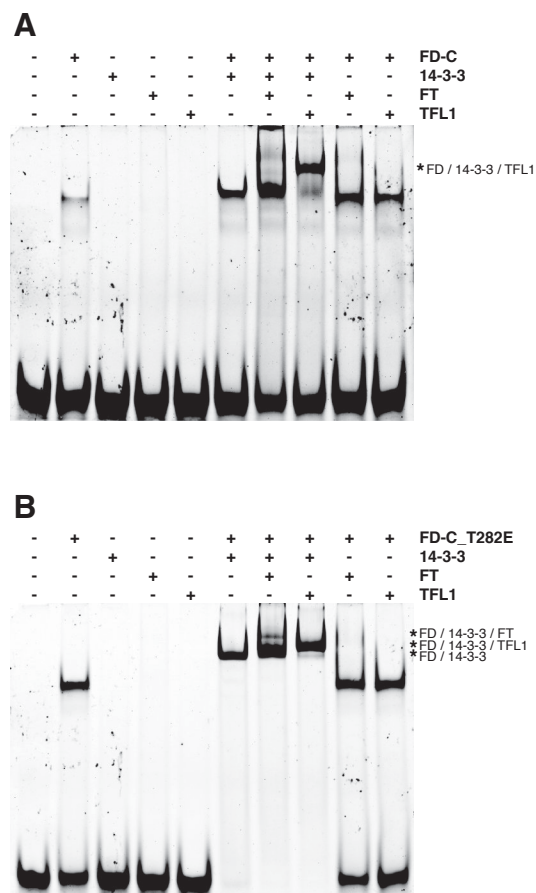


Figure 2. The C-terminal part of FD (FD-C) binds to a G-box in the *SEP3* promoter *in vitro*.

(A) Electrophoretic mobility shift assay (EMSA) of the wild-type form of FD-C in combination with 14-3-3v, FT, and TFL1.

(B) EMSA using the phosphomimic version of FD-C (FD-C_T282E) in combination with 14-3-3v, FT and TFL1.

First lanes to the left in (A) and (B) show the free probe without any added proteins. Plus signs (+) above the lanes indicate which proteins were used in a specific EMSA reaction. Asterisk (*) indicates higher order complexes.

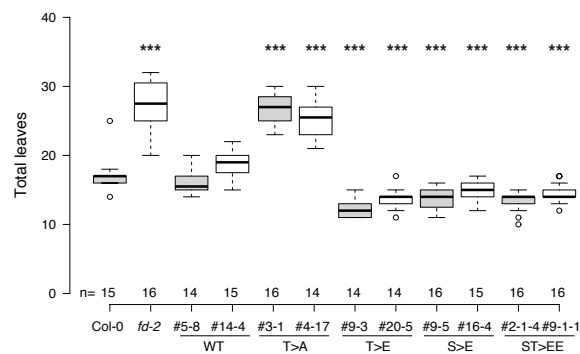


Figure 3. Phosphorylation of FD at threonine 282 (T282) modulates flowering time in *A. thaliana*.

Box plot reporting the flowering time of control plants (Col-0), the *fd-2* mutant, and the *fd-2* mutant transformed with either wildtype (WT) *FD* cDNA under the control of the *FD* promoter (*pFD::FD*), non-phosphorable FD (T>A, *pFD::FD_T282A*), or phosphomimic versions of FD (T>E, *pFD::FD_T282E*; S>E, *pFD::FD-S281E*; ST>EE, *pFD::FD_S281E/T282E*) as number of leaves formed by the main meristem (total leaves). Results are shown for two independent homozygous lines per construct. Number of plants (n) analyzed per genotype is indicated. Statistical significance was calculated using an unpaired t-test compared to Col-0. *** indicates a significance level $p < 0.01$.

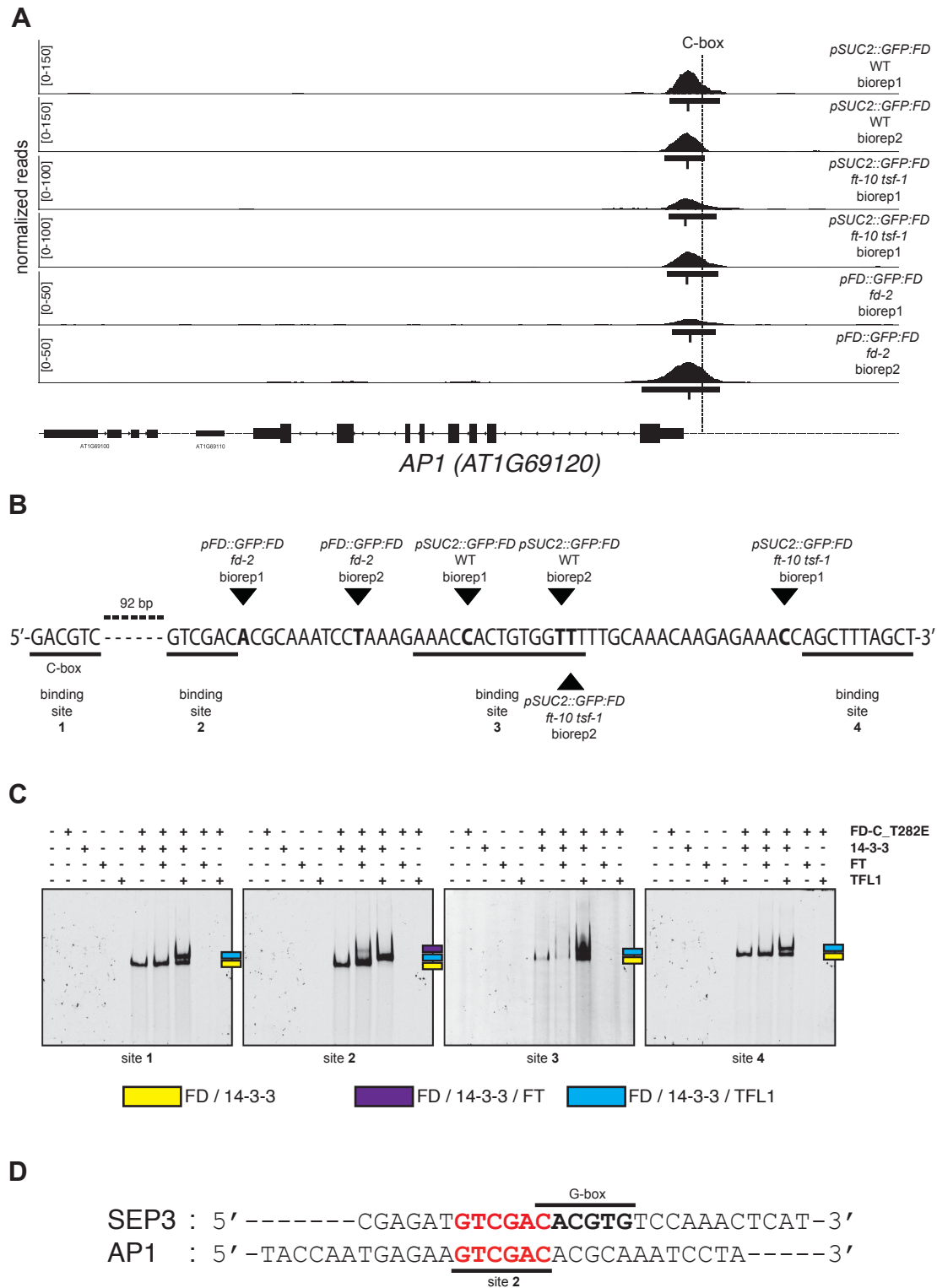


Figure 4. Mapping of the FD binding site in the *AP1* promoter.

(A) Normalized reads from six ChIP-seq experiments mapped on the *AP1* locus. Horizontal bars below the peaks indicate regions of significant enrichment. The position of the summit is indicated for each peak. The C-box previously implicated in FD binding is located upstream (to the right) of peak summits in all six experiments.

- (B)** Nucleotide sequence encompassing the six peak summits shows several palindromic regions representing putative binding sites of FD on the *API* promoter. The distance between the closest potential FD binding site under the ChIP-seq peaks and the C-box is 92 bp. Black triangles indicate the summits of the six separate ChIP-seq experiments. Putative FD binding sites are underlined and numbered from 1 to 4.
- (C)** Electrophoretic mobility shift assay (EMSA) of the phosphomimic version of FD-C (FD-C_T282E) in combination with 14-3-3v, FT and TFL1 using the four putative binding sites reported in panel B. Free probes are not visible because gels were running longer to maximize the distance between shifted probes. Coloured squares indicate shifted probes.
- (D)** Comparison of the probes used for EMSA: the G-box in *SEP3* promoter (Fig. 2) and the binding site 2 in *API* promoter. The putative FD binding site (site 2) in the *API* promoter, which is also conserved in *SEP3* promoter where it overlaps with the G-box, is marked in red.

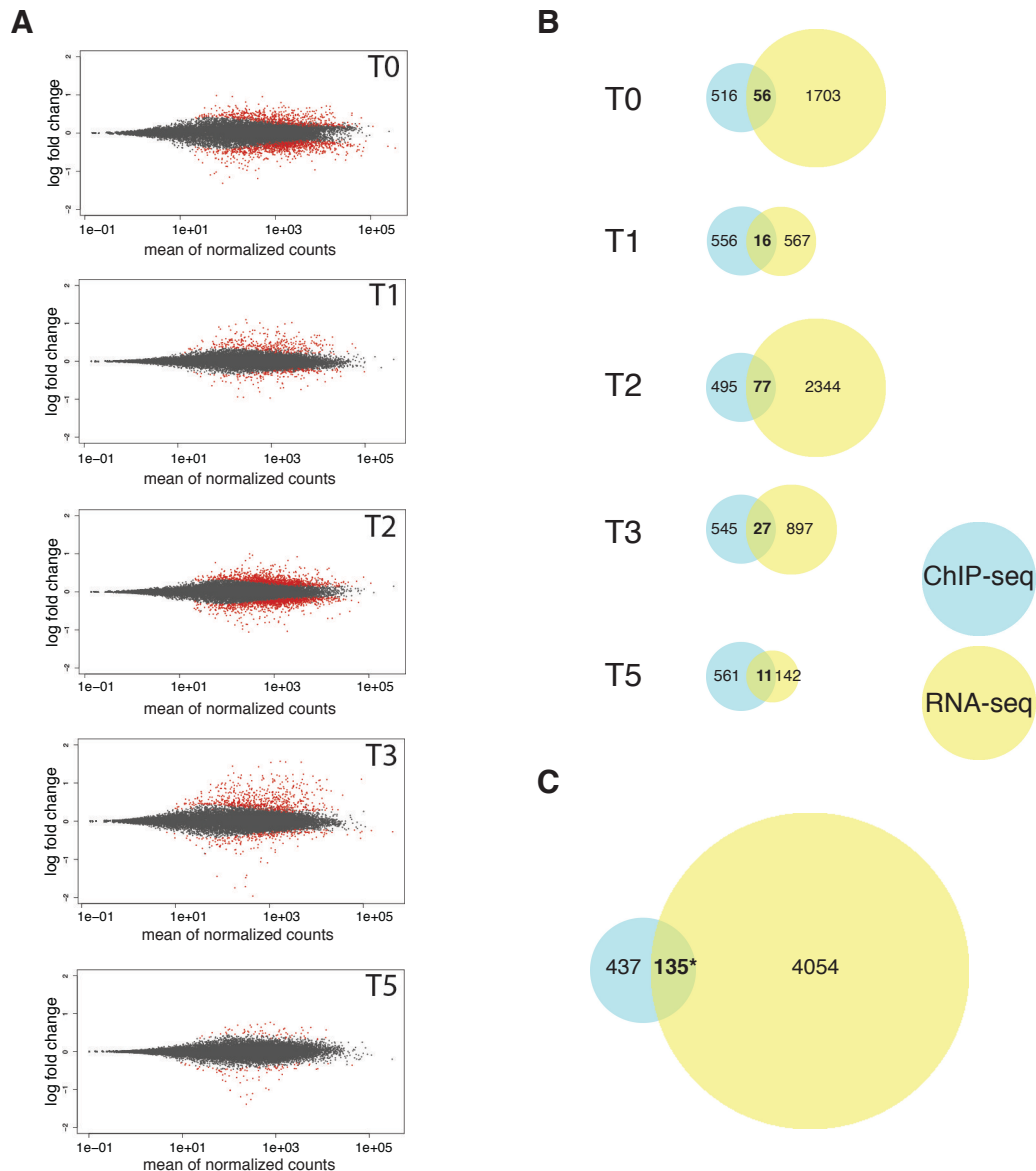


Figure 5. RNA-seq results at the shoot apical meristem.

- (A) Scatter plots of differentially expressed (DE) genes between the *fd-2* mutant and *pFD::GFP-FD fd-2* (control) at 5 time points before and during the transition to photoperiod-induced flowering. T0 – T5 indicate day of sample collection before (T0) and 1, 2, 3, 5 days after shifting plants to long day. Red dots indicate DE genes with a $p_{adj} < 0.1$.
- (B) Venn diagrams showing the overlap between 572 unique FD target genes identified by ChIP-seq and DE genes found by RNA-seq at the SAM at five time points before (T0) and during (T1 – T5) the transition to flowering.
- (C) Venn diagram showing the overlap between 572 unique FD target genes identified by ChIP-seq at the SAM (two biological replicates) and genes found to be differentially expressed at the SAM by RNA-seq at least at one time point (T0, T1, T2, T3, T5; three biological replicates per time point). A total of 135 genes were classified as putative direct targets of FD. Statistical significance was calculated using the Fisher's exact test. Asterisk (*) indicates a significance level $p = 1.03E-07$.

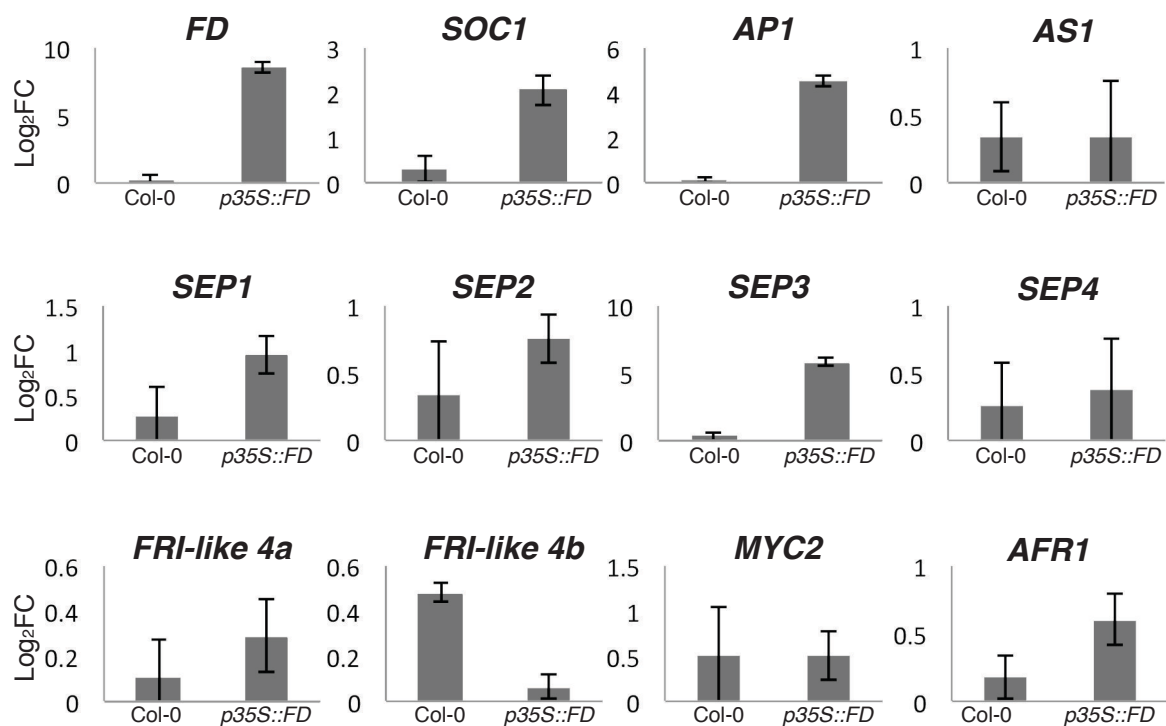


Figure 6. Validation of FD targets in Col-0 and *p35S::FD*.

RT-qPCR analysis of 12 putative direct targets of FD. RNA was isolated from 15-20 7-day-old Col-0 and *p35S::FD* seedlings. Error bars represent \pm SD from three biological replicates.

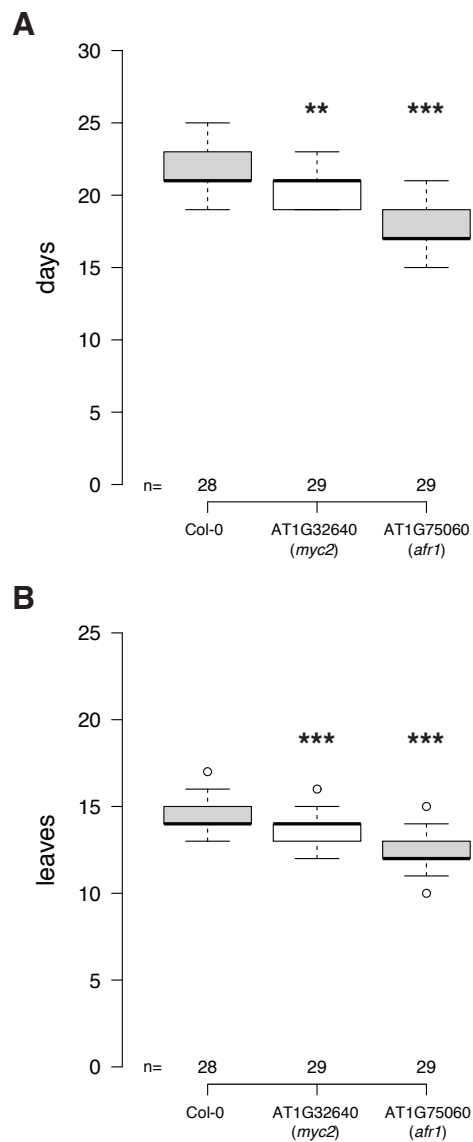


Figure 7. Flowering time of *myc2* and *afr1*.

Flowering time of homozygous *myc2* and *afr1* T-DNA insertion lines was scored as days to flowering (A) and total leaves (B). Number (n) of plants per genotype is indicated. Statistical significance was calculated using an unpaired t-test compared to Col-0. *** and ** indicate a significance level of $p < 0.01$ and $p < 0.05$, respectively. Unfilled circles represent outliers.